Clays and Clay Minerals, Vol. 63, No. 6, 443–456, 2015.

MEASURING THE LAYER CHARGE OF DIOCTAHEDRAL SMECTITE BY O–D VIBRATIONAL SPECTROSCOPY

Artur Kuligiewicz[1], Arkadiusz Derkowski[1,*], Katja Emmerich[2], George E. Christidis[3], Constantinos Tsiantos[4], Vassilis Gionis[4], and Georgios D. Chryssikos[4,*]

[1] Institute of Geological Sciences, Polish Academy of Sciences, ul. Senacka 1, 31-002 Krakow, Poland
[2] Competence Center for Material Moisture (CMM) and Institute of Functional Interfaces (IFG), Karlsruhe Institute of Technology, Hermann-von-Helmholtz-Platz 1, D-76344 Eggenstein-Leopoldshafen, Germany
[3] School of Mineral Resources Engineering, Technical University of Crete, Chania, Greece 73100
[4] Theoretical and Physical Chemistry Institute, National Hellenic Research Foundation, 48 Vass. Constantinou Ave., Athens, Greece 11635

Abstract—Layer charge (LC) is a fundamental property of smectite but its measurement remains challenging and tedious to apply on a high-throughput basis. The present study demonstrates that the position of a sharp, high-energy O–D stretching band of adsorbed D_2O (νO–D, at ~2686–2700 cm^{-1}), determined by infrared spectroscopy, correlates with LC and provides a simple method for its measurement. Twenty nine natural dioctahedral smectites and 14 reduced-charge montmorillonites with LC determined previously by different methodologies were saturated with D_2O and examined by attenuated total reflectance infrared spectroscopy (ATR-IR). The samples included smectites in Mg, Ca, Na, Li, K, and Cs forms and covered the full range of the smectite LC (0.2 to 0.6 *e* per formula unit). Statistically significant correlations were found between νO–D and LC values determined with each of the two main methods of LC determination: the structural formula method (R^2 = 0.96, σ = 0.02, ~0.2 < LC < 0.6) and the alkylammonium method (R^2 = 0.92, σ = 0.01, 0.27 < LC < 0.37). These correlations were based on Li- and Na-saturated smectites, respectively, but other cationic forms can be employed provided that the exchangeable cations are of sufficiently high hydration enthalpy (*e.g.* Mg^{2+} or Ca^{2+}, but not K^+ or Cs^+). The new method is fast, low-cost, implemented easily in laboratories equipped with ATR-FTIR, and applicable to samples as small as ~5 mg.

Key Words—ATR, D_2O, Infrared Spectroscopy, Layer Charge, Smectite.

INTRODUCTION

Layer charge in smectite

The Clay Minerals Society (CMS) Nomenclature Committee defines smectite as a group of 2:1 phyllosilicates with layer charge (LC) between ~0.2 and 0.6 negative elementary charge per $O_{10}(OH)_2$ formula unit (p.f.u.; Güven, 1988; Guggenheim *et al.*, 2006). Layer charge is defined as "the total negative charge deviation from an ideal, unsubstituted dioctahedral or trioctahedral composition" (CMS Nomenclature Committee, 2015). Layer charge controls many properties of smectite, such as the cation exchange capacity (CEC), water adsorption, rheological behavior, *etc*. (*e.g.* Laird, 1999; Harvey and Lagaly, 2006; Laird, 2006; Christidis *et al.*, 2006; Ferrage *et al.*, 2007; Tertre *et al.*, 2015). For these reasons, LC is a key property to determine when characterizing smectite.

Fast and accurate LC determination of smectite remains a challenge. In turn, the way LC is measured influences the specific terminology developed to describe LC in a manner that may be confusing. A portion of the measured smectite charge that is caused by heterovalent, octahedral or tetrahedral substitutions (as in the aforementioned CMS definition of layer charge) is referred to as 'permanent.' Charge originating from OH groups developed at the edges of the 2:1 layer and local structural defects depends on pH and is referred to as 'variable.' The term 'total charge' is, therefore, used hereafter to describe the sum of permanent and variable charges, whereas the term 'charge' is used without specifying charge origin or location. On a purely geometrical basis, the terms 'interlayer charge,' 'basal charge,' and 'edge charge' are used when referring to a charge present in the interlayer, on basal surfaces, and on edges of 2:1 layers, respectively. Although the terms 'variable charge' and 'edge charge' refer to very similar portions of total charge, they may not be directly interchangeable (Kaufhold, 2006; Delaverhne *et al.*, 2015).

Layer-charge measurement methodology

Various methods have been developed to measure the charge of smectites. These involve a chemical analysis and/or CEC measurement of pure, monomineralic smectite fractions (Čícel and Komadel, 1994; Laird, 1994; Christidis, 2008); the exchange with alkylammonium cations of different chain lengths (Lagaly and Weiss, 1969; Ruehlicke and Kohler, 1981; Lagaly,

* E-mail address of corresponding author:
ndderkow@cyf-kr.edu.pl; gdchryss@eie.gr
DOI: 10.1346/CCMN.2015.0630603

1981, 1994; Olis *et al.*, 1990; Dohrmann *et al.*, 1999; Wolters *et al.*, 2009); or the saturation of smectite with particular inorganic cations solvated by polar liquids in combination with X-ray diffractometry (XRD; Christidis and Eberl, 2003). Spectroscopic methods have also been applied to a suspension of smectite in cationic dye solutions (Bujdák, 2006) or to smectites saturated with ammonium cations (Petit *et al.*, 1998).

Structural formula methods (SFM) aim to calculate the deviations from the ideal, unsubstituted dioctahedral or trioctahedral compositions, distributing analyzed elements on the basis of certain assumptions (Stevens, 1946). The SFM are biased by the presence of impurities such as quartz, opal, and feldspars. Interference from impurities can be avoided with electron microprobe techniques (Christidis and Dunham, 1993, 1997), which provide the range of LCs in smectite particles but, inevitably, add to the complexity of the measurement. Furthermore, SFM can be influenced by the presence of non-exchangeable, non-structural cations (Kaufhold *et al.*, 2011), variable charges, and local domains of different octahedral occupancy (*cf.* Wolters *et al.*, 2009).

The alkylammonium method (AAM) probes only the interlayer charge density (Lagaly, 1994). The original methodology returns an entire LC distribution based on the specific conformation of different long-chain alkylammonium cations. Smectite LC is then calculated as a mean value of the LC distribution. The measurement, however, can be influenced by uncertainties in the packing of the alkylammonium cations in the interlayer and by particle-size effects (Laird *et al.*, 1989; Laird, 1994). Additionally, the AAM method is labor intensive, time consuming, and requires a relatively large quantity of sample (>1 g). Modifications of AAM proposed by Olis *et al.* (1990) and Dohrmann *et al.* (1999) aimed to reduce these drawbacks.

The comparison of charge values obtained with SFM and AAM is not straightforward because these methods are based on different assumptions, they are subject to different types of error, and they measure different portions of total charge (*e.g.* Laird, 1994; Kaufhold *et al.*, 2002; Kaufhold, 2006; Christidis, 2008; Kaufhold *et al.*, 2011). The AAM returns lower charge values than the SFM-based or calibrated methods (Laird, 1994; Kaufhold, 2006; Wolters *et al.*, 2009; Kaufhold *et al.*, 2011). Laird (1994) and Kaufhold (2006) have demonstrated experimentally that SFM- and AAM-derived charges are correlated linearly, but that linearity may also depend on the aspect ratio of the smectite crystallites (Delavernhe *et al.*, 2015).

Whereas SFM and AAM provide a value of the layer charge directly and do not require independent calibration, all other LC determination methods involve calibration against one of the two or, with certain assumptions, against the CEC. For example, the XRD-based method developed by Christidis and Eberl (2003) probes only the interlayer charge density and was calibrated against SFM charges. This method is, however, limited to smectites with charge greater than 0.39 p.f.u. The infrared spectroscopic method of Petit *et al.* (1998) correlated CEC with the relative integrated intensity of the ν_4 NH_4^+ bending envelope against the Si−O stretching envelope in a NH_4-exchanged smectite. In combination with a Li^+ fixation pretreatment, this method can provide an additional estimate of charge location (octahedral *vs*. tetrahedral; Petit *et al.*, 2006). This method can be applied to small samples (<5 mg) but is sensitive to the presence of silicate impurities. The electronic spectra of cationic dyes such as methylene blue (Bujdák, 2006; Czímrerová *et al.*, 2006; Pentrák *et al.*, 2012) and rhodamine 6G (Bujdák *et al.*, 2003, 2004) proved to be very sensitive indicators of LC changes in clays, although mostly on a qualitative level.

Water molecules as a probe for smectite surface

Whereas some of the aforementioned probes of layer charge are extrinsic, water is a ubiquitous and intrinsic probe of the surface of clay minerals (Sposito *et al.*, 1983; Johnston *et al.*, 1992; Xu *et al.*, 2000; Schoonheydt and Johnston, 2006; Johnston, 2010). A recent infrared spectroscopic study of D_2O-saturated smectites (Kuligiewicz *et al.*, 2015) reported that the position of the high-frequency O−D stretching band observed at 2680−2695 cm^{-1} (hereafter, νO−D, corresponding to an O−H band of H_2O at 3620−3635 cm^{-1}) seemed to correlate linearly with total charge. The vibrational spectra of adsorbed water (as D_2O) have, therefore, the potential to be adapted for a quick and reliable determination of layer charge in smectites. The high-frequency νO−D band, first described by Farmer and Russell (1964) and Russell *et al.* (1970), was assigned to the stretching modes of so-called "free O−D" ("dangling mode") groups of D_2O molecules positioned in the vicinity of the siloxane surface and nearly perpendicular to the plane of basal oxygen atoms (Figure 1; Russell *et al.*, 1970; Suquet *et al.*, 1977). This interpretation is supported by the observations of high-frequency O−H stretching bands of H_2O at the interfaces with hydrophobic phases such as silica (Jena and Hore, 2010), tetrachloromethane (Scatena *et al.*, 2001), or at water−vapor interfaces (Sovago *et al.*, 2009; Tian and Shen, 2009), where corresponding bands were assigned to the dangling O−H. In the case of the smectite−water interface, the bond strength and the stretching frequency of this dangling O−H (O−D) bond are probably controlled by the entire basal charge, regardless of the charge origin from the octahedral or tetrahedral sheet (Kuligiewicz *et al.*, 2015; *cf.* Farmer and Russell, 1971; Suquet *et al.*, 1977).

The aim of the present work was to develop a new method of layer-charge determination by further testing the correlation of νO−D with LC on a large number of dioctahedral smectite samples with charge determined previously by broadly accepted techniques. The

https://doi.org/10.1346/CCMN.2015.0630603 Published online by Cambridge University Press

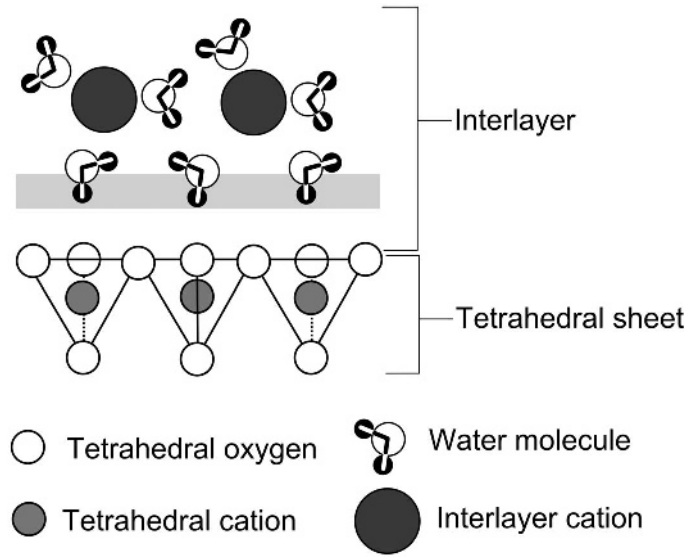

Figure 1. Schematic orientation of water molecules in the vicinity of the basal oxygen plane of a smectite 2:1 layer. The oriented dangling O–D bonds at the water–smectite interface (shaded zone) are involved in the νO–D band, as suggested by Russell *et al.* (1970), Suquet *et al.* (1977), and Kuligiewicz *et al.* (2015). Distances and atomic radii not to scale.

differences between particular charge-measurement reference methods have been discussed extensively in the literature (*e.g.* Mermut, 1994; Laird, 1994; Kaufhold *et al.*, 2002; Kaufhold, 2006; Christidis, 2008; Wolters *et al.*, 2009; Kaufhold *et al.*, 2011; Kaufhold and Dorhmann, 2013) and are beyond the scope of the present study.

MATERIALS AND METHODS

Samples

A collection of 29 natural smectites in various cationic forms and fourteen reduced-charge Li-montmorillonites (RCMs) were examined. The samples studied were grouped in four sets (Table 1):

(A) Fine fractions (<1 μm and finer) thoroughly separated from six smectite reference samples from the Source Clays Repository of The Clay Minerals Society, which included montmorillonites (SAz-2, SCa-3, SWy-2), beidellites (SbCa-1, SbId-1), and a nontronite/ferric-smectite (SWa-1). The same specimens were studied previously by Kuligiewicz *et al.* (2015) and were included here in additional cationic forms for comparison purposes. The total layer charge for this set was determined on XRD-pure smectites (except SbId-1, where minor kaolinite content was subtracted virtually) from the Na content of the Na-exchanged smectite fraction measured by flame photometry after conventional acid digestion (Kuligiewicz *et al.*, 2015). The total charge estimation method applied followed the general SFM definition.

(B) Fifteen natural dioctahedral smectites (<0.2 μm fractions, Na-exchanged) from the study of Wolters *et al.* (2009). Those authors reported the charges of the same specimens by the AAM (Lagaly, 1994), a simplified alkylammonium method (AAOM; Olis *et al.*, 1990), and SFM (Stevens, 1946).

(C) Six montmorillonite samples (SAz-1, SWy-1, SCa-3, STx-1, Woburn, Kinney; <2 μm size fractions) originally used in the study of Christidis and Eberl (2003) and two clay fractions (<2 μm) of bentonites from Cyprus (FEOG and Skouriotissa, referred to hereafter as SK; Christidis, 2006). Both SFM charges and charges calculated by the method of Christidis and Eberl (2003; CEM) were reported by Christidis and Eberl (2003), Christidis (2006), and Skoubris *et al.* (2013). The spectroscopic data reported here were obtained from the Li forms of these fractions (Skoubris *et al.*, 2013).

(D) A series of 13 portions of Li-SAz-1 (<2 μm fraction) montmorillonite subjected to increasing charge reduction by heating for 24 h at 60–180ºC from the study of Skoubris *et al.* (2013). These samples were labeled Li-SAz1-xxx, where xxx denotes the heating temperature. The total charge of these samples was measured with CEM for temperatures up to 135ºC (Skoubris *et al.*, 2013). An additional set of charges for the whole sample set was calculated by multiplying the SFM charge of the unheated material by the % reduction of the CEC upon heating, reported by Skoubris *et al.* (2013).

Mid-infrared spectroscopy

The infrared (IR) spectra of all samples were collected in the 4000–580 cm^{-1} range on two FTIR instruments (Equinox 55 by Bruker Optics, Ettlingen, Germany and Nicolet 6700 by Thermo Scientific, Waltham, Massachusetts, USA) with three different single-reflection diamond Attenuated Total Reflectance

https://doi.org/10.1346/CCMN.2015.0630603 Published online by Cambridge University Press

Table 1. Positions of the sharp, high-frequency O−D stretching band, νO−D, and layer charge of the smectite samples used in the present study.

Set	Sample	Charge location[1]	Interlayer cation	νO−D (cm^{-1})	1σ (cm^{-1})	Layer charge (p.f.u.)		
						SFM[2]		
			Mg	2686.2	0.5			
			Ca	2686.0	0.5			
	SAz-2	O	Na	2686.0	0.5	0.52		
			K	2688.5	0.5			
			Cs	2690.0	0.5			
			Mg	2685.1	0.5			
			Ca	2686.1	0.5			
	SCa-3	O	Na	2686.2	0.5	0.51		
			K	2687.7	0.5			
			Cs	2689.4	0.5			
			Ca	2685.5	0.5			
	SbCa-1	T	Na	2684.5	0.5	0.50		
			K	2687.2	0.5			
A			Mg	2688.8	0.5			
			Ca	2689.3	0.5			
	SbId-1	T	Na	2689.3	0.5	0.39		
			K	2690.6	0.5			
			Cs	2691.6	0.5			
			Mg	2691.8	0.5			
			Ca	2691.8	0.5			
	SWy-2	O/T	Na	2692.4	0.5	0.36		
			K	2692.3	0.5			
			Cs	2693.2	0.5			
			Mg	2691.7	0.5			
			Ca	2692.1	0.5			
	SWa-1	O/T	Na	2692.9	0.5	0.31		
			K	2693.7	0.5			
			Cs	2691.4	1			
						SFM[3]	AAM[4]	AAOM[5]
	2LP	O/T		2692.3	0.2	0.37	0.28	0.29
	3, 7thMayo	O/T		2691.0	0.2	0.42	0.30	0.31
	4JUP	T/O		2692.1	0.2	0.37	0.29	0.30
	5MC	O/T		2692.1	0.4	0.40	0.28	0.28
	6GPC	O/T		2690.4	0.2	0.45	0.33	0.34
	7EMC	O/T		2693.5	0.4	0.40	0.28	0.29
	8UAS	O		2689.0	0.2	0.48	0.34	0.33
B	14TR03	O	Na	2686.5	0.2	0.47	0.37	0.38
	17GR02	O/T		2692.5	0.2	0.38	0.29	0.30
	19USA02	O/T		2690.9	0.2	0.39	0.30	0.31
	21D01	O/T		2691.2	0.2	0.42	0.29	0.31
	28SB	O/T		2688.3	0.2	0.47	0.36	0.39
	31BAR 3	O		2690.4	0.2	0.41	0.32	0.32
	32Volclay	O/T		2693.7	0.2	0.39	0.27	0.27
	33CA	O/T		2690.9	0.2	0.42	0.30	0.30
						SFM[6]	CEM[7]	
	Li-SAz-1	O		2686.9	0.2	0.56	0.55	
	Li-SWy-1	O/T		2693.7	0.2	0.36	0.39	
	Li-Kinney	O		2687.4	0.2	0.49	0.53	
	Li-SK	T/O		2689.6	0.2	0.48	0.50	
C	Li-FeOG	O	Li	2692.9	0.3	0.39	0.39	
	Li-SCa-3	O		2686.9	0.2	0.60	0.60	
	Li-STx-1	O/T		2691.1	0.2	0.44	0.44	
	Li-Woburn	O/T		2692.5	0.3	0.42	0.43	

https://doi.org/10.1346/CCMN.2015.0630603 Published online by Cambridge University Press

Table1 (*contd.*)

Set	Sample	Charge location[1]	Interlayer cation	νO–D (cm^{-1})	1σ (cm^{-1})	Layer charge (p.f.u.)	
						SFM[6]	CEM[7]
	Li-SAz1-60			2687.2	0.2	0.54	0.54
	Li-SAz1-80			2687.7	0.2	0.54	0.53
	Li-SAz1-100			2689.3	0.2	0.52	0.50
	Li-SAz1-105			2689.3	0.2	0.49	0.46
	Li-SAz1-110			2690.6	0.2	0.47	0.44
	Li-SAz1-115			2691.3	0.2	0.44	0.44
D	Li-SAz1-120	O	Li	2694.0	0.3	0.39	0.42
	Li-SAz1-125			2694.4	0.3	0.37	0.40
	Li-SAz1-130			2695.2	0.4	0.31	0.39
	Li-SAz1-135			2696.4	0.5	0.26	0.39
	Li-SAz1-140			2697.3	0.5	0.24	N.A.[8]
	Li-SAz1-160			2697.6	0.6	0.22	N.A.[8]
	Li-SAz1-180			2699.0	0.7	0.19	N.A.[8]

[1] O: Octahedral, T: tetrahedral
[2] Total charge from Na content of Na-exchanged pure smectites (Kuligiewicz *et al.*, 2015; SFM equivalent)
[3] Total charge by structural formula method (SFM) of Stevens (1946)
[4] AAM – alkylammonium method (Lagaly, 1994)
[5] AAOM – simplified alkylammonium method (Olis *et al.*, 1990)
[6] Total charge recalculated from SFM data of unheated sample and CEC reduction of RCM (SFM equivalent);
[7] CEM – XRD method of Christidis and Eberl (2006).
[8] The method could not be applied
Available charges were compiled from Kuligiewicz *et al.* (2015), set A; Wolters *et al.* (2006), set B; Christidis and Eberl (2003), Christidis (2006), and Skoubris *et al.* (2013), set C; Skoubris *et al.* (2013), set D.

(ATR) accessories, employed with their pressure tips removed (DuraSampl IR II by SensIR Technologies, presently Smiths Detection, Edgewood, Maryland, USA; Golden Gate by Thermo Scientific, Waltham, Massachusetts, USA; and MIRacle by PIKE Technologies, Madison, Wisconsin, USA). The wavenumber accuracy of both spectrometers is better than 0.05 cm^{-1} (typically <0.03 cm^{-1}). All spectra were measured at room temperature by averaging 100 scans at 4 cm^{-1} resolution, ($\Delta\nu$ = 2 cm^{-1}). Detailed sample handling and data processing parameters were given by Kuligiewicz *et al.* (2015). Briefly, a few drops of sonicated smectite suspensions in D_2O (99.9 atom% D, Sigma-Aldrich Chemie GmbH, Steinheim, Germany) were deposited on the ATR crystal, covered with a custom-made cup as in Bukas *et al.* (2013), and purged with N_2 of purity better than 99.999 vol.% (<5 ppm H_2O) until a dry ~10 μm thick film was created in good contact with the ATR element. Subsequently, the cap was flushed with N_2 gas enriched with D_2O vapor to 60–80% (±2%) relative humidity (RH) using a custom-made gas blending setup equipped with a calibrated hygrometer. The sample was first equilibrated at ~60% RH (D_2O) for at least 15 min in order to remove traces of H_2O or HDO. Subsequently, 5–10 spectra were collected in the 60 to 80% RH (D_2O) range. This range was chosen because the νO–D value is stable between 60 and 80% RH (figure 7 of Kuligiewicz *et al.*, 2015). Absorbance (ATR) maxima were determined for each spectrum from the 2nd derivative minima calculated with a Savitzky-Golay algorithm (13 point smoothing) using the *Opus*™ software by Bruker (Ettlingen, Germany). The reported values of νO–D (Table 1) represent the average from 5–10 spectra with errors given as one standard deviation (1σ).

RESULTS

The spectra of D_2O-saturated samples display structural O–H stretching bands in the region 3750 to 3500 cm^{-1} (Figure 2). O–D stretching and bending bands are at 2800–2200 cm^{-1}, and ~1200 cm^{-1}, respectively, originating from the adsorbed D_2O (Farmer and Russell, 1964; Russell *et al.*, 1970; Kuligiewicz *et al.*, 2015). A trace HDO bending mode could be observed at ~1450 cm^{-1} and was employed to test the progress of the H/D exchange (Figure 2). The O–D stretching envelope included the high-frequency sharp band (Figure 2, inset) with νO–D in the 2685–2700 cm^{-1} range (Table 1). Because this work investigates the systematics of νO–D following Kuligiewicz *et al.* (2015), the vibrational features of the aluminosilicate network (*e.g.* Madejová *et al.*, 2002; Madejová, 2003; Zviagina *et al.*, 2004; Gates, 2005 and references therein) are not discussed here.

Samples from set A were examined against charges derived from the quantitative analysis of Na in the Na forms (Table 1, Figure 3). This is an extension of a

https://doi.org/10.1346/CCMN.2015.0630603 Published online by Cambridge University Press

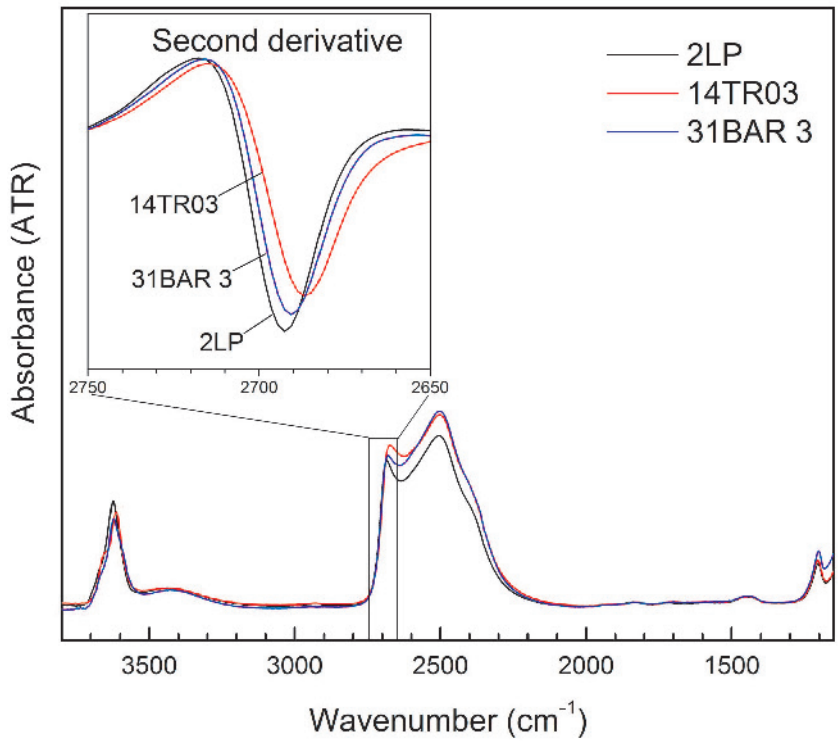

Figure 2. Examples of the IR spectra of D_2O-saturated dioctahedral smectites in the 3800−1150 cm^{-1} range. Three representative samples from set B are shown. The inset illustrates the determination of νO−D from the 2nd derivative spectra.

similar correlation by Kuligiewicz *et al.* (2015) with additional cationic forms. Values of νO−D in the available Mg, Ca, and Na forms differed by 2σ or less (Table 1, Figure 3), and, therefore, could be fitted with a single linear regression equation with R^2 = 0.92. In contrast, the corresponding Cs forms exhibited a narrower distribution of νO−D values with a very weak dependence on charge, whereas the K forms occupy intermediate positions between Cs and the other cation forms (Figure 3). The values of νO−D for different cation forms converge toward the low-charge limit.

The dependence of νO−D on SFM-based layer charge for sets A−C (Table 1, excluding the K and Cs forms of set A) illustrated that linear correlations could be established for all sets, but the quality of the fit is variable (R^2 = 0.70−0.92) and depends on the method of charge determination (Figure 4). Strong correlations were found between νO−D and AAM (R^2 = 0.92) and AAOM (R^2 = 0.84) charges, available for set B (Figure 5). A comparison of R^2 coefficients for different trendlines available for sets A−C revealed that the SFM-based correlation for set B was considerably weaker than either the corresponding AAM-based correlations or the SFM-based correlations for the other sets (Figures 4, 5).

Finally, set D, based on the charge-reduced Li-SAz-1 montmorillonite, exhibited the largest shifts of νO−D toward ~2700 cm^{-1} upon increase of the temperature of the charge-reduction treatment (Figure 6). Above ~120ºC, this shift was accompanied by a pronounced decrease in intensity of the sharp D_2O band. As a result of decreasing D_2O content, νO−D could not be measured for samples heated above 180ºC (Figure 6). The correlation between νO−D and the CEC-derived total charges based on Skoubris *et al.* (2013) for set D was excellent (Figure 7, R^2 = 0.98). The R^2 for set D was greater than for all other sample sets, mostly due to the greatly expanded range of charges (and frequencies) probed down to ~0.2 p.f.u. (and up to ~2700 cm^{-1}). Notably, the trend line of set D (originating from the same parent sample) could not be distinguished from that of set C (independent samples), suggesting that a common regression of νO−D against SFM-based charges can be applied for both Li-exchanged sample sets, regardless of their origin and structure (R^2 = 0.96; Figure 7). For the same sample set D, CEM charges were in good agreement with the CEC-derived SFM data but deviated from the SFM trend line as the layer charge approached the lower limit of CEM (~0.4 p.f.u.; Figure 7).

DISCUSSION

Charge prediction

The experimental results implied that strong correlations could be obtained between νO−D and either type of charge reference data (SFM or AAM). Some variability in the intercept and slope of the different SFM-based regressions was attributed to the different corrections or assumptions involved in the calculation of

https://doi.org/10.1346/CCMN.2015.0630603 Published online by Cambridge University Press

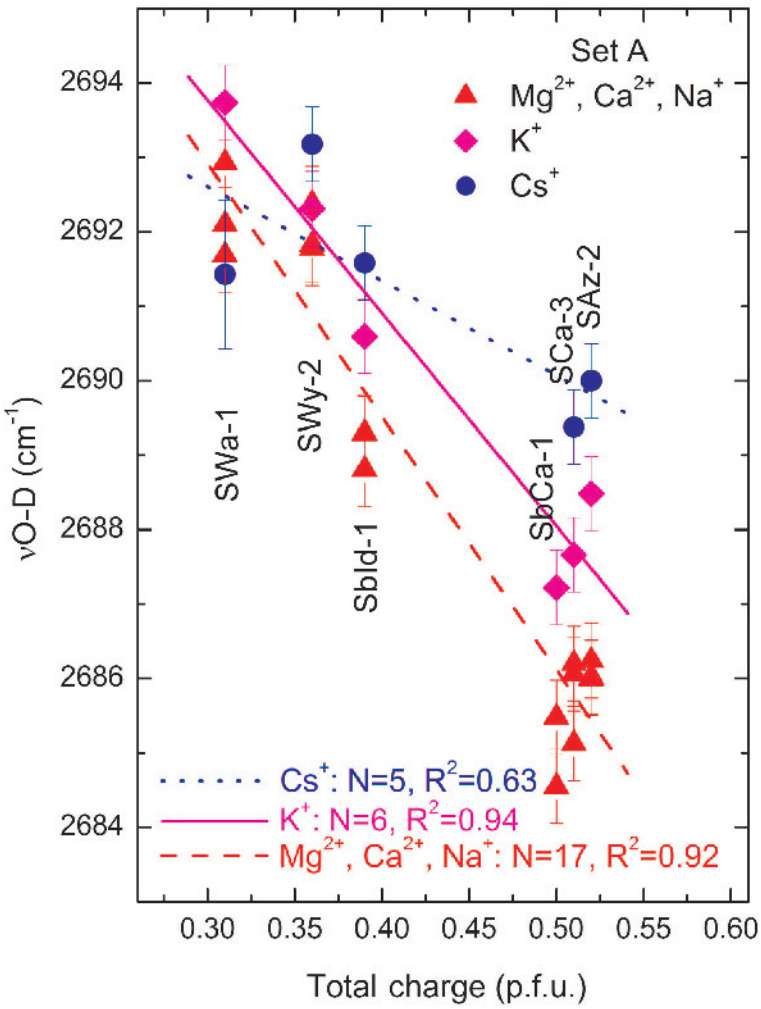

Figure 3. Relationship between νO–D and total charge determined for set A in different cationic forms (Na, Ca, and Cs from Kuligiewicz *et al.*, 2015).

structural formulae in the reference methods and, to a lesser extent, to the different interlayer cations (Figure 4). Validation procedures can be employed to spot outliers in the literature data: *e.g.* removing Kinney montmorillonite from set C using SFM charges, would improve R^2 from 0.89 (Figure 4) to 0.97.

Any of the correlations between νO–D and SFM or AAM charges can be converted into an equation for layer-charge prediction (Figures 4, 5, 7). The two strongest linear correlations for the prediction of SFM- or AAM-based charges were derived from sets C + D and B, respectively (Table 2, Figure 8). In both

Table 2. Linear regression parameters for the prediction of layer charge on the basis of νO–D.
LC = **p** + **q**(νO–D – 2686)

	Set B Na form (AAM)	Sets C and D Li form (SFM)
p	0.38±0.01	0.60±0.01
q	−0.015±0.001	−0.030±0.001
R^2	0.92	0.96
Number of samples	15	21
Charge range (p.f.u.)	0.27–0.37	~0.2–0.6
1σ	0.01	0.02

https://doi.org/10.1346/CCMN.2015.0630603 Published online by Cambridge University Press

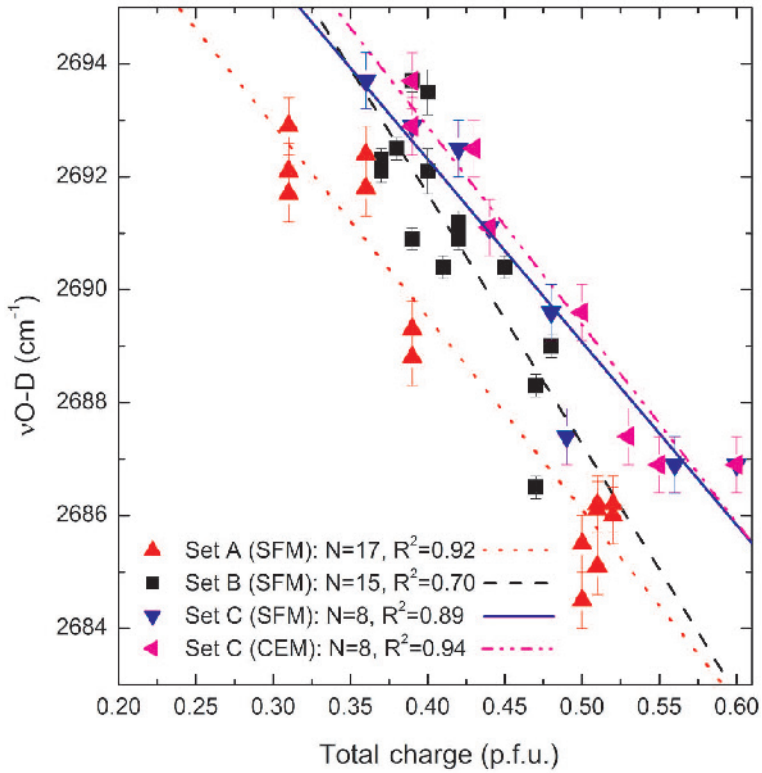

Figure 4. Correlation between νO−D and SFM-based total layer charge for sample sets A−C. Only the Mg, Ca, and Na forms are presented for Set A. CEM charges for set C were included for comparison.

equations, the independent variable was written as (νO−D − 2686) in order to increase the variance of the frequency datasets. The offset value of 2686 cm^{-1} was chosen on the basis of the Li-exchanged sets C and D as the closest integer wavenumber to the high-charge νO−D limit of a smectite definition: 0.6 p.f.u.

The calculated regression equations enabled the prediction of charge as deduced from either SFM or AAM in the ~0.2−0.6 and 0.27−0.37 p.f.u. ranges, with standard deviations of 0.02 and 0.01 p.f.u., respectively (Table 2). These predictions were based specifically on the ATR infrared spectra of D_2O-saturated samples and the determination of the position of the sharp high-frequency mode of D_2O from 2nd derivative analysis. The combination of spectral resolution (4 cm^{-1}), data spacing ($\Delta\nu$ = 2 cm^{-1}), and Savitzky-Golay filter parameters for the calculation of 2nd derivatives (13 point smoothing) used in the present study were optimized previously by Kuligiewicz *et al.* (2015) to balance between resolution and signal-to-noise ratio requirements. A change in these parameters is feasible, but could affect the values of the regression coefficients (Table 2) and, therefore, may require recalibration or calibration transfer.

The regressions for the prediction of SFM and AAM charges (Table 2) were based on the spectra of homo-ionic Li- and Na-exchanged smectites, respectively. This choice was dictated by the availability of sample sets with independent and self-consistent reference charges. The spectroscopic prediction of SFM and AAM charges of an unknown smectite would strictly imply the preparation of the same cationic forms as in the relevant regression. Nevertheless, the study of set A has provided evidence that νO−D is nearly identical in the Na, Ca, and Mg forms of the same smectite (Figure 3; *cf.* Kuligiewicz *et al.*, 2015). This result implies that the choice of interlayer cation has a small effect on the prediction of the charge from νO−D, as long as its hydration enthalpy is high enough to keep the interlayers filled with D_2O and allow for undisrupted D_2O-basal surface interactions.

Influence of interlayer cation and smectite charge location

The negligible effect that the common interlayer cations (Na^+, Ca^{2+}, and Mg^{2+}) have on the value of νO−D is well explained by the assignment of this band to the dangling O−D bonds of interlayer D_2O. In a hydrated smectite, these bonds point away from the strongly hydrogen-bonded D_2O in the interlayer and towards the weakly charged basal surfaces (Figure 1; *cf.* Russell *et al.*, 1970; Suquet *et al.*, 1977). As such, their bond-length and associated vibrational energy are most sensitive to the density of the basal charge and not to the bonding of the hydrated interlayer cations. This is in contrast to the position of the bending mode of interlayer

https://doi.org/10.1346/CCMN.2015.0630603 Published online by Cambridge University Press

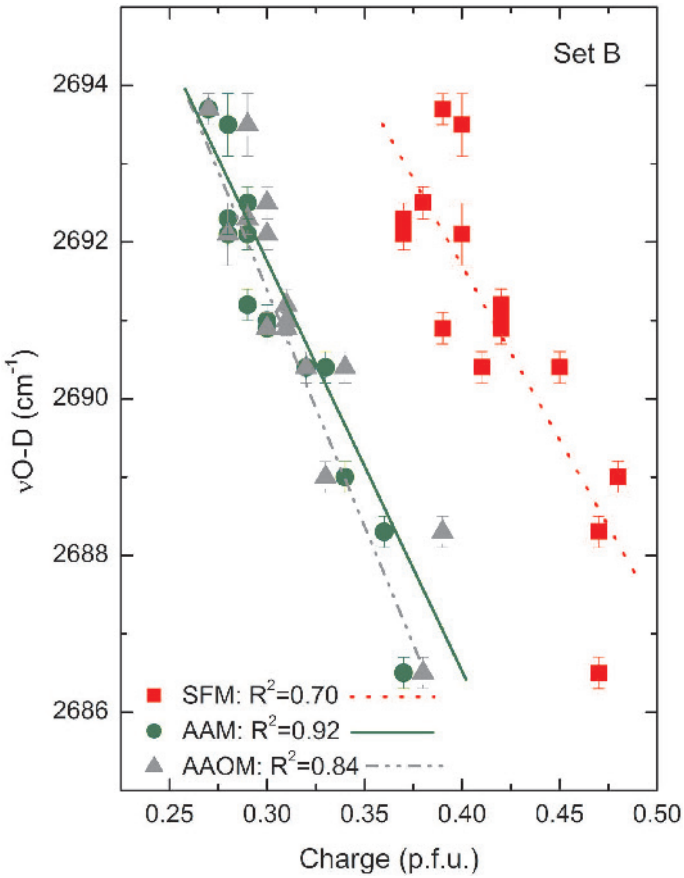

Figure 5. Correlation between νO–D and smectite charges measured with different methods by Wolters *et al.* (2009) for set B. SFM total charges were calculated according to Stevens (1946), AAM and AAOM interlayer charges were calculated after Lagaly (1994) and Olis *et al.* (1990), respectively. Each trend line was derived using 15 samples (*cf.* table 6 of Wolters *et al.*, 2009).

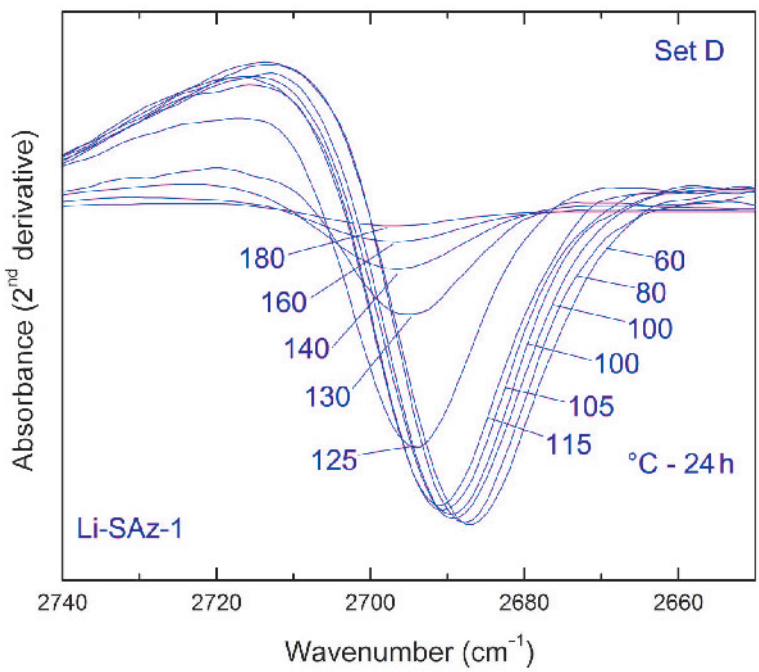

Figure 6. Second derivative of νO–D infrared absorbance for set D. The numbers indicate the heating temperature of Li-SAz-1.

https://doi.org/10.1346/CCMN.2015.0630603 Published online by Cambridge University Press

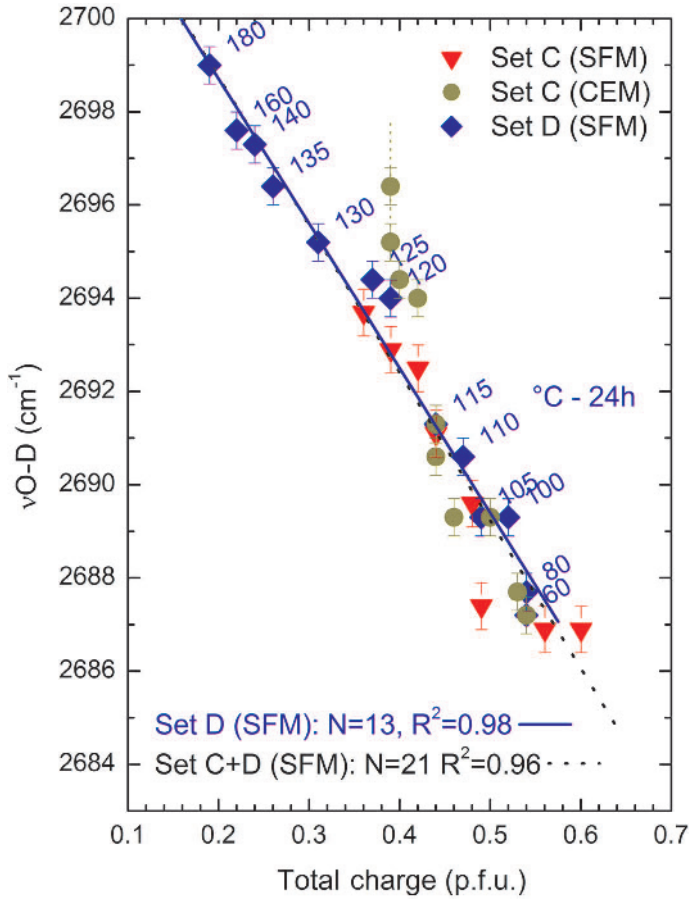

Figure 7. The νO−D *vs.* total charge calculated for sets C and D with SFM (set D: based on CEC reduction). CEM charges for set C are included for comparison. The numbers indicate the heating temperature of SAz-1.

H_2O (D_2O) at ~1630 (~1200) cm^{-1} and the broad stretching envelope at ~3400 (~2500) cm^{-1}, which are cation-dependent (Farmer and Russell, 1966; Johnston *et al.*, 1992; Bishop *et al.*, 1994; Madejová *et al.*, 2002; Kuligiewicz *et al.*, 2015).

The K- and Cs-exchanged smectites are less suitable for LC prediction, especially towards the high-charge limit where the direct interaction of K^+ and Cs^+ with the siloxane surfaces occurs (Eberl *et al.*, 1986; Onodera *et al.*, 1998; Skiba, 2013). The greater the basal charge, the greater the attraction of Cs^+ (or K^+) ions to charged basal oxygen atoms of the tetrahedral sheet. Binding a cation to the basal surface leads to local charge neutralization and, in extreme cases, to the collapse of the interlayer (*cf.* Christidis and Eberl, 2003; Ferrage *et al.*, 2005, 2007; Skiba, 2013). In this case, a high-charge portion of the charged surface will not be available to H_2O (D_2O) and, thus, it would not be probed by νO−D. Hence, the high-charge Cs-saturated smectites would behave as smectites with lower charge, leading to the shift of νO−D to higher wavenumbers (Figure 3). In agreement with the experimental data (Table 1, set A; Figure 3), an increase of νO−D from Mg-, Ca-, or Na- to K- and Cs-exchanged smectite is expected to be most pronounced at the high-charge end because charge heterogeneity tends to increase with charge (Christidis and Eberl, 2003). Such a mechanism explains the similarity of the νO−D values in low-charge smectites regardless of the cationic form (Figure 3). Having intermediate hydration enthalpy, K^+ is bonded directly to fewer high-charge domains in the first shell of the siloxane surface than Cs^+, leaving more surface available to the D_2O probe.

Perhaps counter-intuitively, the νO−D values were found to be independent of charge location (tetrahedral *vs.* octahedral; Table 1), which implies that charges predicted on the basis of νO−D would also be unaffected by charge location. The sample sets A−C included dioctahedral smectites with a variable fraction of tetrahedral charge, including almost pure beidellite and montmorillonite end-members. In contrast, charge in set D was controlled by an octahedral-charge neutralization mechanism that involves Li^+-migration and fixation. None of these factors introduced a measurable bias on νO−D. Samples 5MC, 2LP, and 4JUP (set B) had identical AAM charges and νO−D (0.28±0.01 p.f.u. and

https://doi.org/10.1346/CCMN.2015.0630603 Published online by Cambridge University Press

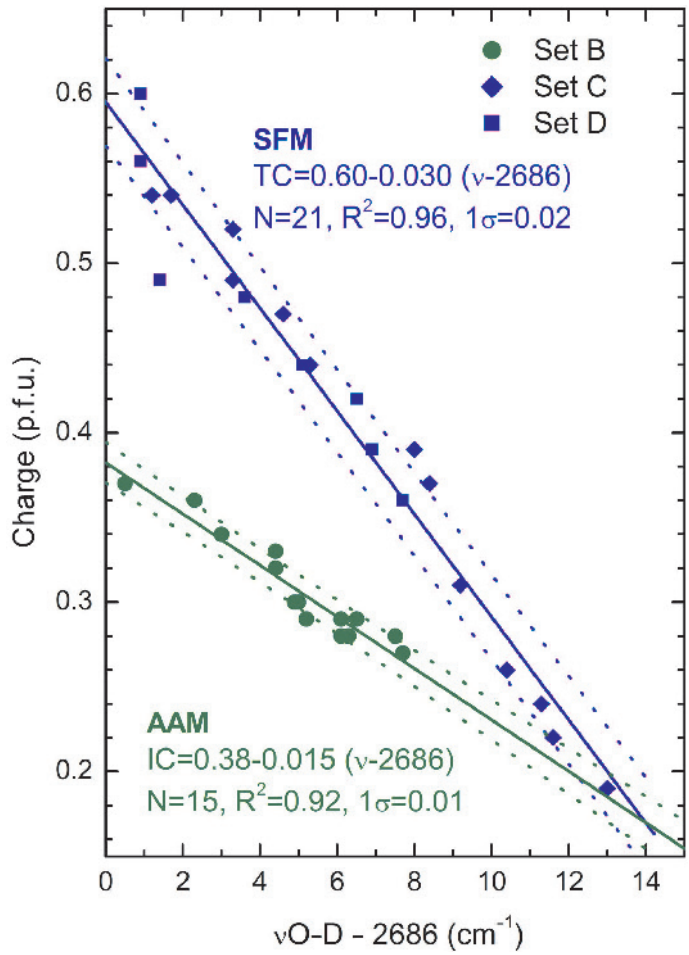

Figure 8. Regressions for the prediction of AAM-based charges (set B, Na-exchanged) and SFM-based charges (sets C+D, Li-exchanged). Both trend lines intercept at the charge value of ~0.2 p.f.u. Dotted lines present 68% prediction bands. IC – interlayer charge; TC – total charge.

2692.2±0.1 cm^{-1}, Table 1) despite the very different fractions of beidellitic charge (13, 24, and 62%, respectively; Wolters *et al.* (2009)). Similarly, Li-Tx-1 (set C) and the Li-SAz-1-115 (set D) had identical SFM charges and νO–D (0.44 p.f.u. and 2691.2±0.1 cm^{-1}, Table 1) despite the obviously different origin of their layer charges.

Other factors influencing layer-charge measurement by the O–D method

The charge predicted from νO–D is essentially the part of the total charge that is spread onto the basal surfaces of the water-accessible interlayers of smectite. In this sense, the proposed spectroscopic method is an interlayer-sensitive technique, conceptually similar to AAM or CEM, but based on the isotopic H/D exchange of H_2O, a ubiquitous and intrinsic constituent of smectite. Smectites are heterogeneous with sample-specific layer-charge distribution that can be probed in detail by AAM (Lagaly, 1994) and, in a coarser manner, by CEM (Christidis and Eberl, 2003). Individual νO–D contributions from layers of different charge could not be resolved spectroscopically. Hence, the O–D method yields a charge averaged over all water-accessible interlayers of all particles in the sample. This average is not necessarily identical to the average layer charge. Collapsed layers, should they exist (*cf.* Ferrage *et al.*, 2005, 2007), would not be probed by D_2O. Similarly, the νO–D of interstratified illite-smectite (Cetin and Huff, 1995; Środoń *et al.*, 2009) or kaolinite-smectite (Cuadros and Dudek, 2006; Dudek *et al.*, 2006) minerals would only reflect the charge of the smectitic component.

Both AAM- and SFM-based charges are highly correlated to νO–D; therefore, these two types of layer charge are linearly related to each other. Similar conclusions were reached by Laird (1994) and Kaufhold (2006). Interestingly, the two types of charge measurement converge at the low-charge limit of LC (Figure 8): a value of νO–D equal to 2699 cm^{-1} would correspond to essentially identical SFM- and AAM-type charges (0.21±0.02 and 0.19±0.01, respectively), which coincides with the low-charge limit in the definition of

https://doi.org/10.1346/CCMN.2015.0630603 Published online by Cambridge University Press

smectite (*cf.* Laird, 1994). Detailed discussion of reasons for discrepancies between AAM and SFM is, however, beyond the scope of the present work.

CONCLUSIONS

The linear relationship between the position of the dangling O–D stretching mode in the FTIR spectra of D_2O-saturated smectites and their layer charge (Kuligiewicz *et al.*, 2015) was confirmed on various sample sets with charges determined by different established techniques. Statistically significant linear correlations were obtained between νO–D and both SFM and AAM charges. These linear regressions can be used for predicting the charge of dioctahedral smectites with high accuracy ($\leqslant$0.02 p.f.u.) and over the entire range of smectite layer charge.

The charge-predicting equations were based on Li- and Na-exchanged smectites (SFM and AAM charges, respectively), which added a cation exchange step prior to the spectroscopic measurement. On the other hand, Ca^{2+} and Mg^{2+}, in addition to Na^{+}, are the most common cations in sedimentary environments and the most predominant exchangeable cations on clay surfaces (*e.g.* Odom, 1984; Dohrmann *et al.*, 2012). The present results suggest that interlayer cations of relatively high hydration enthalpy such as Na^{+}, Ca^{2+}, and Mg^{2+} do not bias the νO–D values (Figure 3). On such a basis, a precise estimate of layer charge can probably be obtained directly from smectites in their natural cationic forms. More accurate charge determinations would require samples in the same cationic form as those used to establish the prediction equation.

The stretching energy of the dangling O–D bond of adsorbed D_2O probes the basal/interlayer charge, *i.e.* the portion of charge referred to as permanent charge or layer charge. The proposed method and prediction equations provide an average charge of the smectite layers that are hydrated and accessible to H/D exchange. The prediction equations are based on band positions rather than intensities and, therefore, do not require normalization. The method is insensitive to the presence of anhydrous impurities. The measurement is fast and requires small amounts of sample (~5 mg), as well as relatively common instrumentation. As such, the proposed O–D method is an appealing low-cost alternative for determining the layer charge of dioctahedral smectite in high-throughput applications, such as the mapping of bentonite deposits (*e.g.* Christidis, 2001; Christidis *et al.*, 2006; Christidis and Huff, 2009). On a more fundamental research front, this can be the technique-of-choice for determining the charge of expandable layers in mixed-layered clay minerals such as illite-smectite, chlorite-smectite, and kaolinite-smectite.

In its present form, the method was tested on natural and reduced-charge dioctahedral smectites. Further effort is needed to extend this approach to additional sample sets, such as synthetic smectites, vermiculites, and trioctahedral smectites. Preliminary results on a synthetic high-charge saponite (Kuligiewicz *et al.*, 2015) and beidellites (Kuligiewicz *et al.*, unpublished data), suggest that an approach similar to that proposed can be developed for trioctahedral and synthetic phases.

ACKNOWLEDGMENTS

The authors thank J. Kieć, M. Zielińska, and M. Lempart for technical assistance. Marek Szczerba is greatly acknowledged for his comments and explanations. The authors also thank the reviewers and editors for valuable comments which improved the manuscript. This project was implemented with financial support from project REGPOT-2011-1 under the European Union 7th Framework Programme, No 285989 (ATLAB) and the IGS-PAS research grant for young scientists ''Dehydration of smectites: a FTIR, TG, and stable isotopes study''. Partial support from project KRHPIS 447963 - Polynano (GSRT, TPCI-NHRF) is acknowledged. This work was performed to partially fulfill the requirements of a Ph.D. thesis by A. Kuligiewicz.

REFERENCES

Bishop, J.L., Pieters, C.M., and Edwards, J.O. (1994) Infrared spectroscopic analyses on the nature of water in montmorillonite. *Clays and Clay Minerals*, **42**, 702–716.

Bujdák, J. (2006) Effect of the layer charge of clay minerals on optical properties of organic dyes. A review. *Applied Clay Science*, **34**, 58–73.

Bujdák, J., Iyi, N., Kaneko, Y., Czímerová, A., and Sasai, R. (2003) Molecular arrangement of rhodamine 6G cations in the films of layered silicates: the effect of the layer charge. *Physical Chemistry Chemical Physics*, **5**, 4680–4685.

Bujdák, J., Iyi, N., and Sasai, R. (2004) Spectral properties, formation of dye molecular aggregates, and reactions in rhodamine 6G/layered silicate dispersions. *Journal of Physical Chemistry B*, **108**, 4470–4477.

Bukas, V.J., Tsampodimou, M., Gionis, V., and Chryssikos, G.D. (2013) Synchronous ATR infrared and NIR-spectroscopy investigation of sepiolite upon drying. *Vibrational Spectroscopy*, **68**, 51–60.

Christidis, G.E. (2001) Formation and growth of smectites in bentonites: a case study from Kimolos Island, Aegean, Greece. *Clays and Clay Minerals*, **49**, 204–215.

Christidis, G.E. (2006) Genesis and compositional heterogeneity of smectites. Part III: Alteration of basic pyroclastic rocks – A case study from the Troodos Ophiolite Complex, Cyprus. *American Mineralogist*, **91**, 685–701.

Christidis, G.E. (2008) Validity of the structural formula method for layer charge determination of smectites: A re-evaluation of published data. *Applied Clay Science*, **42**, 1–7.

Christidis, G. and Dunham, A.C. (1993) Compositional variations in smectites derived from intermediate volcanic rocks. A case study from Milos Island, Greece. *Clay Minerals*, **28**, 255–273.

Christidis, G. and Dunham, A.C. (1997) Compositional variations in smectites. Part II: Alteration of acidic precursors, a case study from Milos Island, Greece. *Clay Minerals*, **32**, 253–270.

Christidis, G.E. and Eberl, D.D. (2003) Determination of layer-charge characteristics of smectites. *Clays and Clay Minerals*, **51**, 644–655.

Christidis, G.E. and Huff, W.D. (2009) Geological aspects and genesis of bentonites. *Elements*, **5**, 93–98.

Christidis, G.E., Blum, A.E., and Eberl, D.D. (2006) Influence

of layer charge and charge distribution of smectites on the flow behaviour and swelling of bentonites. *Applied Clay Science*, **34**, 125–138.

Cetin, K. and Huff, W.D. (1995) Layer charge of the expandable component of illite/smectite in K-bentonite as determined by alkylammonium ion exchange. *Clays and Clay Minerals*, **43**, 150–158.

Čícel, B. and Komadel, P. (1994) Structural formulas of layer silicates. Pp 114–136 in: *Quantitative Methods in Soil Mineralogy* (J.E. Amonette and L.W. Zelazny, editors). Miscellaneous Publications, Soil Science Society of America, Madison, Wisconsin, USA.

Clay Minerals Society Nomenclature Committee (2015) The Clay Minerals Society Glossary for Clay Science, http://www.clays.org/GLOSSARY/Clay_Glossary.htm, access August 25, 2015.

Cuadros, J. and Dudek, T. (2006) FTIR investigation of the evolution of the octahedral sheet of kaolinite-smectite with progressive kaolinization. *Clays and Clay Minerals*, **54**, 1–11.

Czímrerová, A., Bujdák, J., and Dohrmann, R. (2006) Traditional and novel methods for estimating the layer charge of smectites. *Applied Clay Science*, **34**, 2–13.

Delavernhe, L., Steudel, A., Darbha, G.K., Schäfer, T., Schuhmann, R., Wöll, C., Geckeis, H., and Emmerich, K. (2015) Influence of mineralogical and morphological properties on the cation exchange behavior of dioctahedral smectites. *Colloids and Surfaces A: Physicochemical and Engineering Aspects*, **481**, 591–599.

Dohrmann, R., Kaufhold, S., Echle, W., and Meyer, F.M., (1999) Beyond the methylene-blue test: introduction of the Cu(II)-triethylene-tetramine method for smectite estimation in bentonite. Euroclay Meeting, Krakow.

Dohrmann, R., Genske, D., Karnland, O., Kaufhold, S., Kiviranta, L., Olsson, S., Plötze, M., Sandén, T., Sellin, P., Svensson, D., and Valter, M. (2012) Interlaboratory CEC and exchangeable cation study of bentonite buffer materials: II. Alternative methods. *Clays and Clay Minerals*, **60**, 176–185.

Dudek, T., Cuadros, J., and Fiore, S. (2006) Interstratified kaolinite-smectite: Nature of the layers and mechanism of smectite kaolinization. *American Mineralogist*, **91**, 159–170.

Eberl, D.D., Środoń, J., and Northrop H. R. (1986) Potassium fixation in smectite by wetting and drying. Pp 296–326 in: *Geochemical Processes at Mineral Surfaces* (J.A. Davis and K.F. Hayes, editors). American Chemical Society Symposium Series, **323**.

Farmer, V.C. and Russell, J.D. (1964) The infrared spectra of layer silicates. *Spectrochimica Acta*, **20**, 1149–1173.

Farmer, V.C. and Russell, J.D. (1966) The infrared adsorption spectrometry in clay studies Pp. 121–142 in: *Proceedings of 15th National Conference Pittsburgh, Pennsylvania* (S.W. Bailey, editor). Pergamon Press, New York, USA.

Farmer, V.C. and Russell, J.D. (1971) Interlayer complexes in layer silicates: The structure of water in lamellar ionic solutions. *Transactions of the Faraday Society*, **67**, 2737–2749.

Ferrage, E., Lanson, B., Sakharov, B.A., and Drits, V.A. (2005) Investigation of smectite hydration properties by modeling experimental X-ray diffraction patterns: Part I. Montmorillonite hydration properties. *American Mineralogist*, **90**, 1358–1374.

Ferrage, E., Lanson, B., Sakharov, B.A., Geoffroy, N., Jacquot, E., and Drits, V.A. (2007) Investigation of dioctahedral smectite hydration properties by modeling of X-ray diffraction profiles: Influence of layer charge and charge location. *American Mineralogist*, **92**, 1731–1743.

Gates, W.P. (2005) Infrared spectroscopy and the chemistry of dioctahedral smectites. Pp. 126–168 in: *The Application of Vibrational Spectroscopy to Clay Minerals and Layered Double Hydroxides* (J.T. Kloprogge, editor). CMS Workshop Lectures, Vol. **13**, The Clay Minerals Society, Boulder, Colorado, USA.

Guggenheim, S., Adams, J.M., Bain, D.C., Bergaya, F., Brigatti, M.F., Drits, V.A., Formoso, M.L.L., Galán, E., Kogure, T., and Stanjek, H. (2006) Summary of recommendations of nomenclature committees relevant to clay mineralogy: Report of the Association Internationale pour l' Etude des Argiles (AIPEA) Nomenclature Committee for 2006. *Clays and Clay Minerals*, **54**, 761–772.

Güven, N. (1988) Smectites. Pp 497–559 in: *Hydrous Phyllosilicates (Exclusive of Micas)* (S.W. Bailey, editor). Reviews in Mineralogy, **19**, Mineralogical Society of America, Washington, D.C., USA.

Harvey, C. and Lagaly, G. (2006) Conventional applications. Pp. 501–540 in: *Handbook of Clay Science* (F. Bergaya, B.K.G. Theng, and G. Lagaly, editors). Elsevier, Amsterdam.

Jena, C.J. and Hore, D.K. (2010) Water structure at solid surfaces and its implications for biomolecule adsorption. *Physical Chemistry Chemical Physics*, **12**, 14383–14404.

Johnston, C.T. (2010) Probing the nanoscale architecture of clay minerals. *Clay Minerals*, **45**, 245–279.

Johnston, C.T., Sposito, G., and Erickson, C. (1992) Vibrational probe studies of water interactions with montmorillonite. *Clays and Clay Minerals*, **40**, 722–730.

Kaufhold, S. (2006) Comparison of methods for the determination of the layer charge density (LCD) of montmorillonites. *Applied Clay Science*, **34**, 14–21.

Kaufhold, S. and Dohrmann, R. (2013) The variable charge of dioctahedral smectites. *Journal of Colloid and Interface Science*, **390**, 225–233.

Kaufhold, S., Dohrmann, R., Ufer, K., and Meyer, F.M. (2002) Comparison of methods for the quantification of montmorillonite in bentonites. *Applied Clay Science*, **22**, 145–151.

Kaufhold, S., Dohrmann, R., Stucki, J.W., and Anastacio, A.S. (2011) Layer charge density of smectites – closing the gap between the structural formula method and the alkyl ammonium method. *Clays and Clay Minerals*, **59**, 200–211.

Kuligiewicz, A., Derkowski, A., Szczerba, M., Gionis, V., and Chryssikos, G.D. (2015) Revisiting the infrared spectrum of the water-smectite interface. *Clays and Clay Minerals*, **63**, 15–29.

Lagaly, G. (1981) Characterization of clays by organic compounds. *Clay Minerals*, **16**, 1–21.

Lagaly, G. (1994) Layer charge determination by alkylammonium ions. Pp. 1–47 in: *Layer Charge Characteristics of 2:1 Silicate Clay Minerals* (A.R. Mermut, editor). CMS Workshop Lectures, Vol. **6**, The Clay Minerals Society, Aurora, Colorado, USA.

Lagaly, G. and Weiss, A. (1969) Determination of the layer charge in mica-type layer silicates. Pp. 61–80 in: *Proceedings of the International Clay Conference, Tokyo* (L. Heller and N.G. Kaigi, editors), **1**, Israel University Press, Jerusalem.

Laird, D.A. (1994) Evalutation of structural formulae and alkylammonium methods of determining layer charge. Pp. 79–103 in: *Layer Charge Characteristics of 2:1 Silicate Clay Minerals* (A.R. Mermut, editor). CMS Workshop Lectures, Vol. **6**, The Clay Minerals Society, Aurora, Colorado, USA.

Laird, D.A. (1999) Layer charge influences on the hydration of expandable 2:1 phyllosilicates. *Clays and Clay Minerals*, **47**, 630–636.

Laird, D.A. (2006) Influence of layer charge on swelling of smectites. *Applied Clay Science*, **34**, 74–87.

Laird, D.A., Scott, A.D., and Fenton, T.E. (1989) Evaluation of

the alkylammonium method of determining layer charge. *Clays and Clay Minerals*, **37**, 41–46.

Madejová, J. (2003) FTIR techniques in clay mineral studies. *Vibrational Spectroscopy*, **31**, 1–10.

Madejová, J., Janek, M., Komadel, P., Herbert, H.-J., and Moog, H.C. (2002) FTIR analyses of water in MX-80 bentonite compacted from high salinary salt solution systems. *Applied Clay Science*, **20**, 255–271.

Mermut, A.R. (1994) Problems associated with layer charge characterization of 2:1 phyllosilicates. Pp. 105–123 in: *Layer Charge Characteristics of 2:1 Silicate Clay Minerals* (A.R. Mermut, editor). CMS Workshop Lectures, Vol. **6**, The Clay Minerals Society, Aurora, Colorado, USA.

Odom, I.E. (1984) Smectite clay minerals: properties and uses. *Philosophical Transactions of The Royal Society A*, **311**, 391–409.

Onodera, Y., Iwasaki, T., Ebina, T., Hayashi, H., Torii, K., Chatterjee, A., and Mumura, H. (1998) Effect of layer charge on fixation of cesium ions in smectites. *Journal of Contaminant Hydrology*, **35**, 131–140.

Olis, A.C., Malla, P.B., and Douglas, L.A. (1990) The rapid estimation of the layer charges of 2:1 expanding clays from a single alkylammonium ion expansion. *Clay Minerals*, **25**, 39–50.

Pentrák, M., Czímrerová, A., Madejová, J., and Komadel, P. (2012) Changes in layer charge of clay minerals upon acid treatment as obtained from their interactions with methylene blue. *Applied Clay Science*, **55**, 100–107.

Petit, S., Righi, D., Madejová, J., and Decarreau, A. (1998) Layer charge estimation of smectites using infrared spectroscopy. *Clay Minerals*, **33**, 579–591.

Petit, S., Righi, D., and Madejová, J. (2006) Infrared spectroscopy of NH_4^+-bearing and saturated clay minerals: A review of the study of layer charge. *Applied Clay Science*, **34**, 22–30.

Ruehlicke, G. and Kohler, E.E. (1981) A simplified procedure for determining layer charge by the n-alkylammonium method. *Clay Minerals*, **16**, 305–307.

Russell, J.D., Farmer, V.C., and Velde, B. (1970) Replacement of OH by OD in layer silicates, and identification of vibrations of these groups in infra-red spectra. *Mineralogical Magazine*, **37**, 869–879.

Scatena, L.F., Brown, M.G., and Richmond, G.L. (2001) Water at hydrophobic surfaces: Weak hydrogen bonding and strong orientation effects. *Science*, **292**, 908–912.

Schoonheydt, R. and Johnston, C. (2006) Surface and interface chemistry of clay minerals. Pp. 87–113 in: *Handbook of Clay Science* (F. Bergaya, B.K.G. Theng, and G. Lagaly, editors). Elsevier, Amsterdam.

Skiba, M. (2013) Evolution of dioctahedral vermiculite in geological environments – an experimental approach. *Clays and Clay Minerals*, **61**, 290–302.

Skoubris, E.N., Chryssikos, G.D., Christidis, G.E., and Gionis, V. (2013) Structural characterization of reduced-charge montmorillonites. Evidence based on FTIR spectroscopy, thermal behavior, and layer-charge systematics. *Clays and Clay Minerals*, **61**, 83–97.

Sovago, M., Kramer Campen, R.K., Bakker H.J., and Bonn, M. (2009) Hydrogen bonding strength of interfacial water determined with surface sum-frequency generation. *Chemical Physics Letters*, **470**, 7–12.

Sposito, G., Prost, R., and Gaultier, J.P. (1983) Infrared spectroscopic study of adsorbed water on reduced-charge Na-Li-montmorillonites. *Clays and Clay Minerals*, **31**, 9–16.

Środoń, J., Zeelmaekers, E., and Derkowski, A. (2009) The charge of component layers of illite-smectite in bentonites and the nature of end-member illite. *Clays and Clay Minerals*, **57**, 649–671.

Stevens, R.E. (1946) A system for calculating analyses of micas and related minerals to end members. *U.S. Geological Survey Bulletin*, **950**, 101–119.

Suquet, H., Prost, R., and Pezerat, H. (1977) Water adsorbed by calcium saponite – IR spectroscopy. *Clay Minerals*, **12**, 113–126.

Tertre, E., Delville, A., Pret, D., Hubert, F., and Ferrage, E. (2015) Cation diffusion in the interlayer space of swelling clay minerals – A combined macroscopic and microscopic study. *Geochimica et Cosmochimica Acta*, **149**, 251–267.

Tian, C.S. and Shen, Y.R. (2009) Sum-frequency vibrational spectroscopic studies of water/vapor interfaces. *Chemical Physics Letters*, **470**, 1–6.

Wolters, F., Lagaly, G., Kahr, G., Nueesch, R., and Emmerich, K. (2009) A comprehensive characterization of dioctahedral smectites. *Clays and Clay Minerals*, **57**, 115–133.

Xu, W.Z., Johnston, C.T., Parker, P., and Agnew, S.F. (2000) Infrared study of water sorption on Na-, Li-, Ca-, and Mg-exchanged (SWy-1 and SAz-1) montmorillonite. *Clays and Clay Minerals*, **48**, 120–131.

Zviagina, B.B., McCarty, D., Środoń, J., and Drits V.A. (2004) Interpretation of infrared spectra of dioctahedral smectites in the region of OH-stretching vibrations. *Clays and Clay Minerals*, **52**, 399–410.

(*Received 20 November 2015; revised 20 January 2016; Ms. 1069; AE: J. Madejová*)